NMR Study of the Interaction between the B Domain of Staphylococcal Protein A and the Fc Portion of Immunoglobulin G

Hiroaki Gouda,[‡] Miki Shiraishi,[‡] Hideo Takahashi,[‡] Koichi Kato,[‡] Hidetaka Torigoe,[§] Yoji Arata,[||] and Ichio Shimada*[,‡]

Faculty of Pharmaceutical Sciences, The University of Tokyo, Bunkyo-ku, Tokyo 113, Japan, Water Research Institute, Sengen, Tsukuba, Ibaraki 305, Japan, and Tsukuba Life Science Center, The Institute of Physical and Chemical Research (RIKEN), Tsukuba, Ibaraki 305, Japan

Received April 21, 1997; Revised Manuscript Received October 13, 1997[⊗]

ABSTRACT: The solution structure of the B domain of staphylococcal protein A (FB) complexed with the Fc fragment of immunoglobulin G (IgG) is reported. A previous NMR analysis has shown that in solution FB is composed of a bundle of three α-helices, helix I, helix II, and helix III [Gouda, H., Torigoe, H., Saito, A., Sato, M., Arata, Y., and Shimada, I. (1992) *Biochemistry 31*, 9665−9672]. In contrast, the crystal structure of FB in the FB−Fc complex lacks helix III. Uniformly ^{15}N- and ^{15}N/^{13}C-labeled FB were prepared, and the backbone ^{13}C resonances were assigned. The spectral data obtained in the present study indicated that in solution all three helices including helix III are preserved in the FB−Fc complex. The mode of interaction of FB with the Fc fragment was discussed on the basis of the combined data of hydrogen−deuterium exchange experiments and ^{1}H−^{15}N correlation spectroscopy. It was concluded that a contiguous surface shaped by F14, Y15, E16, L18, and H19 in helix I, and N29, Q33, L35, and K36 in helix II is responsible for the binding.

Protein A, which is a cell wall component of *Staphylococcus aureus*, specifically binds to the Fc[1] portion of immunoglobulin G (IgG) from various mammalian species (*1*). The extracellular part of protein A contains a tandem of 5 highly homologous Fc-binding domains designated as E, D, A, B, and C, each of which comprises about 60 amino acid residues. The C-terminal part is a cell wall binding domain designated as X, which does not bind to the Fc portion and comprises approximately 180 amino acid residues (*2*−*4*).

The three-dimensional structure of the B domain of protein A (FB) bound to the Fc fragment of pooled human IgG has been solved by an X-ray crystallographic analysis at 2.8 Å resolution (*5*). The electron density for the Fc-bound FB was observed for the F6−E48 segment; no structural information was available for the A2−K5 and A49−K59 segments. The crystal data indicated that two antiparallel helical regions, Q10−L18 and E26−D37, exist in the Fc-bound FB. It was also suggested that FB makes two types of contact with the Fc fragment in the crystal.

In a previous study (*6*), we have indicated that FB in solution is composed of a bundle of three α-helices, i.e., helix I (Q10−H19), helix II (E25−D37), and helix III (S42−A55). The solution structure of FB is in marked contrast to the crystal structure, where the S42−E48 segment does not take any ordered structure (*5*). We suggested crystal contacts as a possible cause of this discrepancy (*6*).

The crystal structure was obtained using the FB−Fc complex, whereas the solution structure was that of uncomplexed FB. Therefore, in order to proceed further, we had to determine the solution structure of FB in the FB−Fc complex. Due to the obvious difficulty of treating by NMR the FB−Fc complex with a molecular weight of 60K, we decided to use the chemical shift of ^{13}Cα, which reflects the secondary structure of proteins (*7*).

In order to locate the region which FB utilizes for the binding with the Fc fragment, attempts were made to use ^{1}H−^{15}N correlation spectroscopy in combination with hydrogen−deuterium (H−D) exchange measurements. On the basis of the NMR data obtained, we discuss the mode of the interaction of FB with the Fc fragment.

MATERIALS AND METHODS

Sample Preparation. A synthetic gene for FB has been expressed in *Escherichia coli* (*8*). FB uniformly labeled with ^{15}N ([^{15}N]FB) or ^{15}N and ^{13}C ([^{15}N/^{13}C]FB) was prepared

* Author to whom correspondence should be addressed. FAX: +81-(3)-3815-6540. E-MAIL: shimada@iw-nmr.f.u-tokyo.ac.jp.

‡ The University of Tokyo.

§ The Institute of Physical and Chemical Research.

|| Water Research Institute.

⊗ Abstract published in *Advance ACS Abstracts,* December 15, 1997.

[1] Abbreviations: Fc, fragment composed of the C-terminal halves of the heavy chains of immunoglobulin G; IgG, immunoglobulin G; FB, B domain of staphylococcal protein A; 2D, two dimensional; NMR, nuclear magnetic resonance; H−D, hydrogen−deuterium; HSQC, heteronuclear single-quantum correlation; CT, constant time; HNCA, amide proton to nitrogen to α-carbon correlation; HNCO, amide proton to nitrogen to carbonyl carbon correlation; HN(CO)CA, amide proton to nitrogen to α-carbon (via carbonyl carbon) correlation; HCACO, α-proton to α-carbon to carbonyl carbon correlation; Ha, α-proton; Cα, α-carbon; CO, carbonyl carbon; ppm, parts per million; C_H2, C_H3, constant regions of the C-terminal half of the heavy chain of immunoglobulin; NOE, nuclear Overhauser effect; TPPI, time-proportional phase incrementation; 3D, three dimensional; DANTE, delays alternating with nutation for tailored excitation; INEPT, insensitive nuclei enhancement by polarization transfer; DSS, sodium 2,2-dimethyl-2-silapentane-5-sulfonate.

S0006-2960(97)00923-9 CCC: $15.00
Published on Web 01/06/1998

by growing the bacteria in M9 minimal medium using $^{15}NH_4Cl$ as the sole nitrogen source or $^{15}NH_4Cl$ and [$^{13}C_6$] glucose as the sole nitrogen and carbon sources, respectively. FB was isolated and purified as previously described (*9*). The Fc fragment of human myeloma protein IgG(κ) Ike-N was also prepared as previously reported (*6*).

NMR Spectroscopy. All three-dimensional triple-resonance experiments, CT-HNCA, CT-HNCO, CT-HN(CO)CA (*10*), and CT-HCACO (*11*), were acquired on a Bruker AMX400 spectrometer using a triple-resonance $^{15}N/^{13}C/^{1}H$ 5-mm probe. Measurements were made using about 1 mM [$^{15}N/^{13}C$]FB solution at pH 5.0 and 30 °C in H_2O or D_2O. The proton carrier was fixed at the water resonance frequency. The carbon carrier frequencies were set as follows: 56 ppm for $^{13}C\alpha$, and 175 ppm for ^{13}CO. The nitrogen carrier frequency was set to 117 ppm. Spectral widths of 1600, 5000, and 1000 Hz were used for ^{15}N, $^{13}C\alpha$, and ^{13}CO, respectively. The States-TPPI method (*12*) was used to achieve quadrature detection in $t1$ and $t2$. The 3D data matrix ($\omega1 \times \omega2 \times \omega3$) contained 64 (complex) × 128 (complex) × 512 (real) data points. A shifted sine-bell function was used in $t1$, $t2$, and $t3$ for resolution enhancement.

$^{1}H-^{13}C$ HSQC (*13*) spectra of free and Fc-bound [$^{15}N/^{13}C$]FBs were recorded at pH 6.0 and 42 °C in D_2O using a Bruker AMX400 spectrometer. A molar ratio of FB to the Fc fragment was 1.0 to 1.0 for the complex. In order to obtain the $^{1}H-^{13}C$ HSQC spectra, constant time evolution (*14*) was used during $t1$ for the free FB, while we performed ^{15}N and ^{13}CO decoupling during $t1$ on the Fc-bound FB, considering the molecular weight of 60K. In both experiments, carbonyl decoupling pulses were applied as hard pulses using an off-resonance DANTE sequence during $t1$. Spectral widths of 5000 and 2200 Hz were used for ^{1}H and ^{13}C, respectively. Data points of 2K were used in the $t2$ dimension, and a total of 128−256 $t1$ points were recorded using the States-TPPI method (*12*). The delay for the $^{1}H-^{13}C$ INEPT portion was set to 1.75 ms for the free FB and 1.2 ms for the Fc-bound FB, which is smaller than $1/4J_{CH}$. The experiments then yielded optimum $^{1}H-^{13}C\alpha$ correlation. $^{1}H-^{15}N$ HSQC spectra were also recorded for the free and Fc-bound [^{15}N]FBs at pH 6.0 and 42 °C in H_2O. Spectral widths of 6000 and 1200 Hz were used for ^{1}H and ^{15}N, respectively. Data points of 1K were used in the $t2$ dimension, and a total of 128−256 $t1$ points were recorded using the States-TPPI method. For yielding the optimum $^{1}H-^{15}N$ correlation, the delay was set to 2.55 ms and 2 ms for the free FB and the Fc-bound FB, respectively.

The data acquired for the free FB were multiplied by a Gauss function in $t2$ and a shifted sine-bell function in $t1$. During the data processing of spectra obtained for the bound FB, we used a stronger Gauss function in $t2$ for the improvement of the signal separation.

For the H−D exchange experiments, $^{1}H-^{15}N$ HSQC spectra were recorded with spectral widths of 6000 Hz for ^{1}H and 1400 Hz for ^{15}N on a JEOL JNM-GSX spectrometer operating at a 500 MHz proton frequency. Data points of 1K were used in the $t2$ dimension, and 32 transients were acquired for each of the 128 $t1$ points. Quadrature detection in $t1$ was accomplished using the method of States et al. (*15*). The measurement time for one spectrum is about 80 min.

Determination of H−D Exchange Rates of Amide Protons. In order to acquire the H−D exchange rates of amide protons in the Fc-bound FB, lyophilized [^{15}N]FB was initially dissolved in an H_2O solution of the Fc fragment at pH 6.0 and 30 °C. The molar ratio of FB to the Fc fragment was 1.0 to 1.0. Under this condition, all of the FB molecules are tightly bound to the Fc fragments. The solution of the FB−Fc complex was diluted with D_2O, and the diluted sample solution was concentrated by ultrafiltration at pH 6.0 and 4 °C. The concentrated solution of the FB−Fc complex was divided into several samples. Each sample was incubated in D_2O for time intervals ranging from 0.5 to 83 h at pH 6.0 and 30 °C for the H−D exchange of the amide protons. The concentration of the FB−Fc complex was ∼0.7 mM. The pH of the sample solution was then adjusted to pH 3.5, where FB was released from the Fc fragment, and the 2D $^{1}H-^{15}N$ HSQC spectrum of the released FB was measured in D_2O. The H−D exchange of the individual amide protons was followed by varying the time of incubation using 2D $^{1}H-^{15}N$ HSQC experiments. In order to determine the exchange rates, plots of the peak volume versus time were fitted to a single exponential decay. A protection factor, $p = k_{free}/k_{bound}$, was finally calculated for each amide proton. In order to obtain the H−D exchange rates in the free FB, the sample preparation was also done in the same way in the absence of the Fc fragment. The $^{1}H-^{15}N$ HSQC spectra then sequentially were measured at pH 6.0 and 30 °C with a time interval of 80 min.

Competitive Binding Assay. A competitive micro-ELISA technique was used in order to study Fc binding of the mutants of FB: F14A and L18A, in which F14 and L18 are replaced by alanine residues, respectively. The wells of a 96-well microtiter plate were coated with 50 mL of human Fc (5 mg/mL) in a phosphate buffer (PBS) at 4 °C overnight. After coating, the plate was washed 3 times with PBS containing 0.1% Tween 20. The wells then were coated with 100 mL of PBS containing 0.1% bovine serum albumin at 37 °C for 90 min in order to block nonspecific binding sites, and washed 3 times with PBS containing 0.1% Tween 20. A protein A reagent conjugated to peroxidase (Kirkegaard & Perry Laboratories Inc.) was diluted 1:10000 in PBS. Serial dilutions of FB and its mutants were also made in PBS. A 1:1 mixture of reagent and protein solutions was added to the well in a total volume of 100 mL, and incubated at 37 °C for 90 min. After a final washing, 100 mL of substrate, 2,2′-azinobis(3-ethylbenzothiazoline-6-sulfonate (Kirkegaard & Perry Laboratories Inc.), was added and incubated for 30 min at room temperature. The absorbance was measured at 405 nm on a microplate reader.

RESULTS

NMR Experiments. In the previous paper, all resonances originating from the amide protons and nitrogens of the backbone of FB except for A2 were assigned (*6*). On the basis of those assignments, the backbone $^{1}H\alpha$, $^{13}C\alpha$, and ^{13}CO resonances were unambiguously assigned by the CT-HNCA, CT-HNCO, CT-N(CO)CA, and CT-HCACO experiments. Figure 1 shows representative planes of CT-HNCA and CT-HN(CO)CA spectra at a fixed ^{15}N ($\omega1$) chemical

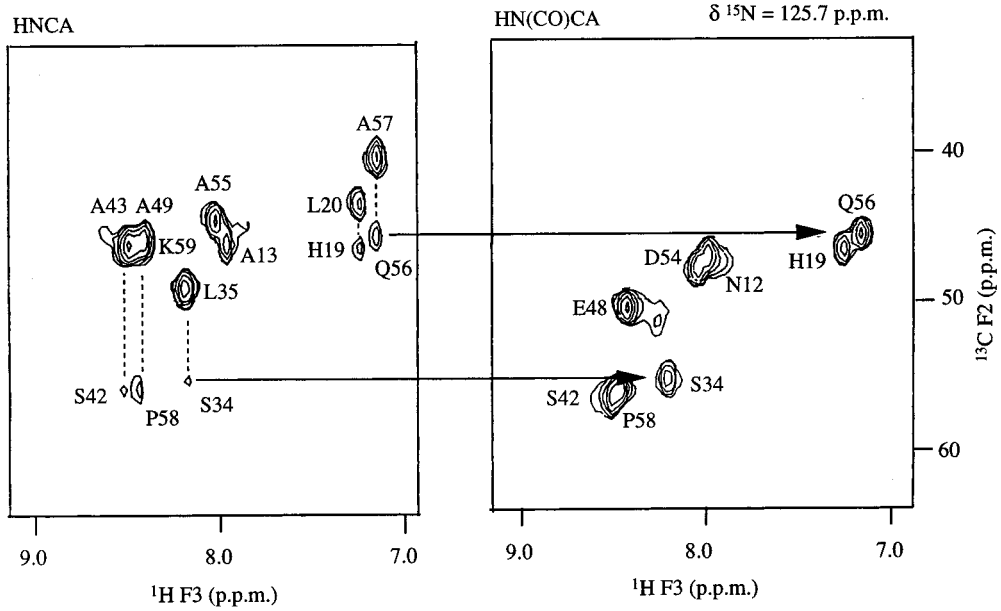

FIGURE 1: Selected $^{13}C(F2)-^{1}H(F3)$ planes at $\delta[^{15}N(F1)] = 125.7$ ppm of CT-HNCA and CT-HN(CO)CA spectra of [$^{15}N/^{13}C$]FB. The intraresidue and interresidue correlations in the HNCA spectrum are connected by the dashed lines with residue assignments. Sequential connectivities for several residues are indicated by the arrows.

shift for the sequential assignment. A set of CT-HNCA and CT-HN(CO)CA spectra was used to link adjacent residues on the basis of their $^{13}C\alpha$ chemical shifts. A complete assignment of the resonances originating from FB in the complex was impossible even by using perdeuterated FB along with ^{2}H decoupling, owing mainly to the fast relaxation of ^{15}N and ^{13}C. Table 1 summarizes the $^{1}H\alpha$, $^{13}C\alpha$, and ^{13}CO chemical shifts of the backbone of free FB observed at pH 5.0 and 30 °C.

Figure 2A,B shows the $^{1}H-^{15}N$ HSQC spectra of [^{15}N]-FB in the absence and presence of Fc, respectively. As shown in Figure 2B, most of the resonances arising from the Fc-bound FB remain at the same positions as observed in the spectrum of the free FB, while several cross-peaks originating from the FB−Fc complex are significantly shifted upon binding to the Fc fragment, compared with the spectrum obtained for the free FB. Therefore, the residues of FB which are affected upon binding Fc are able to be identified. Similar analyses have already been carried out in other Ig-binding proteins to determine the binding site (*16*, *17*). We suggest that the residues Q10, Y15, L18, H19, R28, N29, G30, L35, D37, S40, Q41, S42, A43, and N44 are responsible for the binding to the Fc fragment. $^{1}H-^{15}N$ HSQC spectra can also provide information on the microenvironment of the side chains of the asparagine and glutamine residues. The changes in the chemical shifts of the side-chain resonances originating from N7, Q10, Q11, N12, N29, and Q33 were observed upon binding to Fc (Figure 2B).

Figure 3A,B also shows the $^{13}C\alpha$ regions of the $^{1}H-^{13}C$ HSQC spectra of [$^{15}N/^{13}C$]FB observed in the absence and presence of Fc, respectively. In Figure 3B, while the cross-peaks originating from the bound FB are much broader in line width than those from the free FB, reflecting that the strong dipole−dipole interaction exists at Hα−Cα groups in the complex, the cross-peaks from the bound FB are able to be observed at almost the same chemical shift as in the free FB.

In Figure 3B, the cross-peaks corresponding to T1, A2, D3, N4, K5, K59, and A60 in free FB show narrow line widths even in the complex. It should be noted that all the sharp cross-peaks observed in the complex are due to the N- or C-terminus and that the chemical shifts are almost identical to those observed in the free state. These observations indicate that the N- and C-termini of FB have high mobility even in the complex.

Table 1: $^{1}H\alpha$, $^{13}C\alpha$, and ^{13}CO Chemical Shifts[a] of FB at pH 5.0 and 30 °C

residue	$^{1}H\alpha$	$^{13}C\alpha$	^{13}CO	residue	$^{1}H\alpha$	$^{13}C\alpha$	^{13}CO
T1	3.87	59.8	169.0	F31	4.43	60.8	175.9
A2	4.35	51.2	174.8	I32	3.70	63.1	175.9
D3	4.46	52.5	173.9	Q33	3.90	57.1	176.6
N4	4.53	51.9	173.2	S34	4.24	61.1	174.0
K5	4.14	55.0	174.6	L35	3.74	56.2	175.9
F6	4.99	54.5	175.2	K36	3.97	58.0	177.3
N7	4.70	50.4	173.7	D37	4.42	55.2	175.3
K8	3.95	58.3	176.5	D38	4.90	50.5	171.2
E9	4.07	58.1	177.9	P39	4.48	63.2	176.8
Q10	3.85	57.1	175.7	S40	4.28	59.5	174.5
Q11	3.94	57.1	176.5	Q41	4.59	53.8	174.6
N12	4.58	54.6	175.5	S42	3.72	62.1	172.5
A13	4.04	54.1	176.5	A43	4.09	54.1	179.2
F14	3.80	59.4	174.5	N44	4.49	54.3	176.1
Y15	3.91	60.8	177.2	L45	4.11	56.3	176.6
E16	3.97	58.8	178.4	L46	3.77	56.2	176.2
I17	3.37	64.2	176.1	A47	4.00	53.8	179.4
L18	3.66	55.8	175.2	E48	3.98	57.6	177.1
H19	4.44	54.6	172.7	A49	3.44	53.8	177.6
L20	4.47	51.9	175.8	K50	3.73	58.8	176.9
P21	4.38	63.7	176.3	K51	4.08	58.1	178.0
N22	4.97	51.2	174.3	L52	4.14	56.2	176.4
L23	4.41	52.8	174.7	N53	3.93	56.5	176.2
N24	4.88	49.7	173.9	D54	4.43	55.5	177.0
E25	3.91	58.0	176.2	A55	4.22	52.8	177.5
E26	4.02	58.3	178.7	Q56	4.36	53.6	172.4
Q27	3.86	56.6	177.3	A57	4.32	49.3	173.9
R28	3.76	59.2	175.9	P58	4.41	61.6	175.1
N29	4.38	54.7	176.7	K59	4.29	54.4	173.7
G30	3.75	45.5	174.9	A60	4.11	52.0	180.8

[a] Chemical shifts of ^{1}H and ^{13}C are expressed in ppm relative to DSS and dioxane, respectively.

Determination of H−D Exchange Rates of Amide Protons. In the present study, the H−D exchange experiments of the

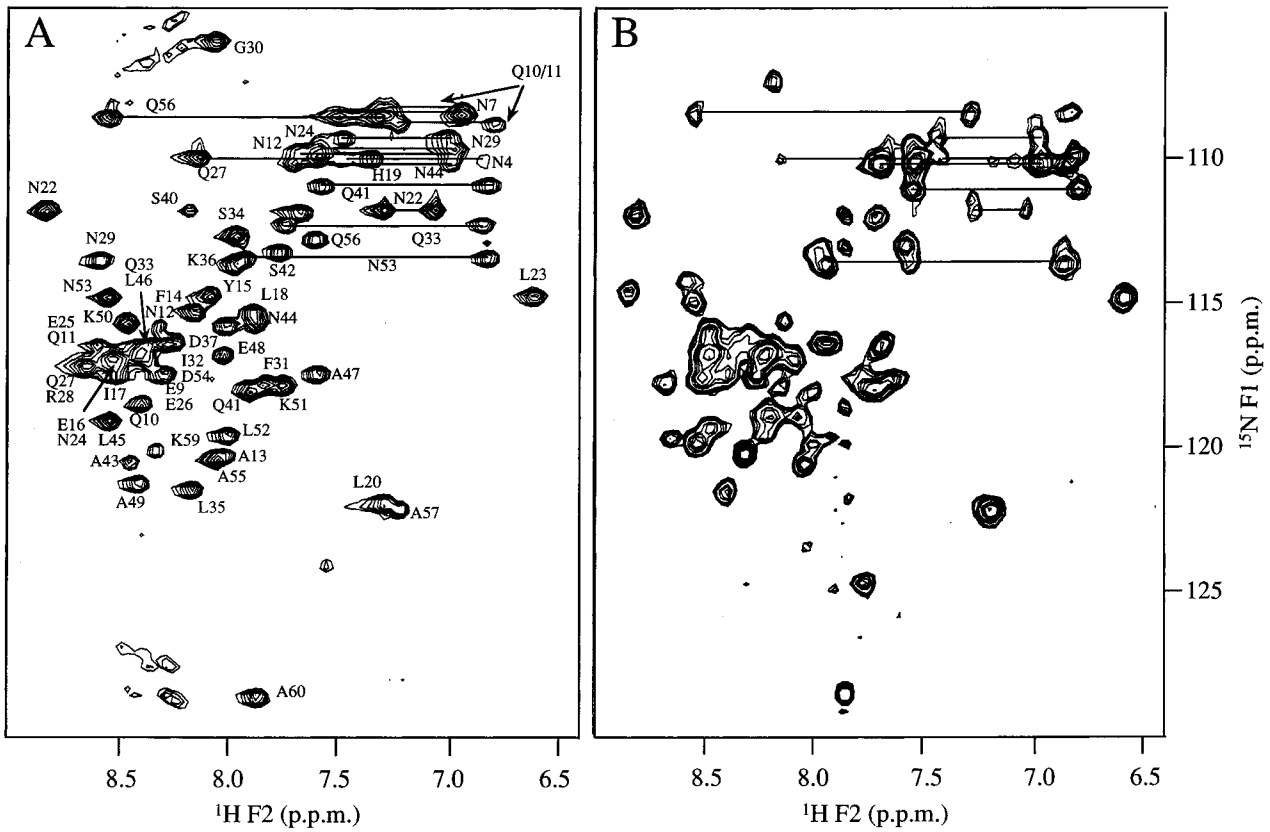

FIGURE 2: ^{1}H−^{15}N HSQC spectra of [^{15}N]FB in the absence (A) and the presence (B) of 1 equiv of Fc at pH 6.0 and 42 °C. ^{1}H−^{15}N correlation peaks are labeled for all resonances in (A). The cross-peaks originating from the side-chain amide groups are connected by solid lines. The resonances originating from the side-chain amide groups of Q10 and Q11 could not be assigned in a site-specific way.

backbone amide protons were carried out at pH 6.0 and 30 °C, where FB was tightly bound to Fc. Under these conditions, the measurements of the H−D exchanges rate became possible for a maximum number of amide protons of the Fc-bound FB. Among the 26 amide protons of FB, for which the exchanges could be followed in the presence of Fc, 22 are located in 1 of the 3 α-helices. The rest of the amide protons originate from turn structures that connect the helices. The H−D exchange rates for the residues of N- and C-terminal segments were too fast to be measured under the conditions used in the present experiment. The H−D exchange rates for I17, L18, I32, L35, A49, and K50 were too slow ($k_{bound} < 7 \times 10^{-5}$ min^{-1}) to be measured in the presence of Fc. Representative curves, which illustrate the quality of the H−D exchange data obtained in the present experiment, are shown in Figure 4. Exponential fits performed for all the experimental curves indicated an average correlation coefficient of 0.97 and a root mean square of 0.04. Figure 5A shows the H−D exchange rates measured in the free (k_{free}) and Fc-bound (k_{bound}) FBs for each amide proton. Protection factors (k_{free}/k_{bound}) are graphically summarized in Figure 5B.

As shown in Figure 5A, most of the residues in helix I give faster H−D exchange rates than those in helices II and III in the free FB, indicating that helix I possesses a lower stability in the absence of Fc. These data might support the results of the fluorescence measurements by using mutant FB where tryptophan residues are introduced in order to investigate the stability and unfolding of FB (*18*). All of the H−D exchange rates of the amide protons of FB measured in the presence of Fc are slower than those observed in the absence of Fc, giving protection factors ranging from 1.3 to >343 (Figure 5B). Of all the measured amide protons, 14 have protection factors greater than 10. These residues correspond to F14−H19 in helix I; N29, I32, Q33, L35, and K36 in helix II; and L46, A49, and K50 in helix III. Especially, the H−D exchange rates for the amide protons of F14, Y15, and E16 were dramatically reduced upon binding to Fc with protection factors larger than 300. L20, N22, L23, R28, F31, S34, D38, L45, A47, E48, K51, and L52 have protection factors less than 8.1.

DISCUSSION

Secondary Structure of the Fc-Bound FB in Solution. In the ^{1}H−^{15}N HSQC spectra in the presence of the Fc fragment (Figure 2B), most resonances of helix III (L45, L46, A47, E48, A49, K50, K51, L52, N53, D54, and A55) are unaffected by the addition of the Fc fragment, indicating that the region corresponding to helix III does not introduce any significant conformational change upon binding to the Fc fragment.

The correlation between ^{13}Cα chemical shifts and the backbone conformation has been confirmed using a number of proteins with known structure (*7*). It has been reported that ^{13}Cα resonances are sensitive to secondary structures of proteins and tend to shift downfield and upfield in α-helices and β-sheets, in reference to the chemical shifts observed in the random coil, respectively (*7*). In order to discuss the secondary structure of the Fc-bound FB in solution, we used the ^{13}Cα region in the ^{1}H−^{13}C HSQC spectrum (Figure 3). It should be noted that none of the

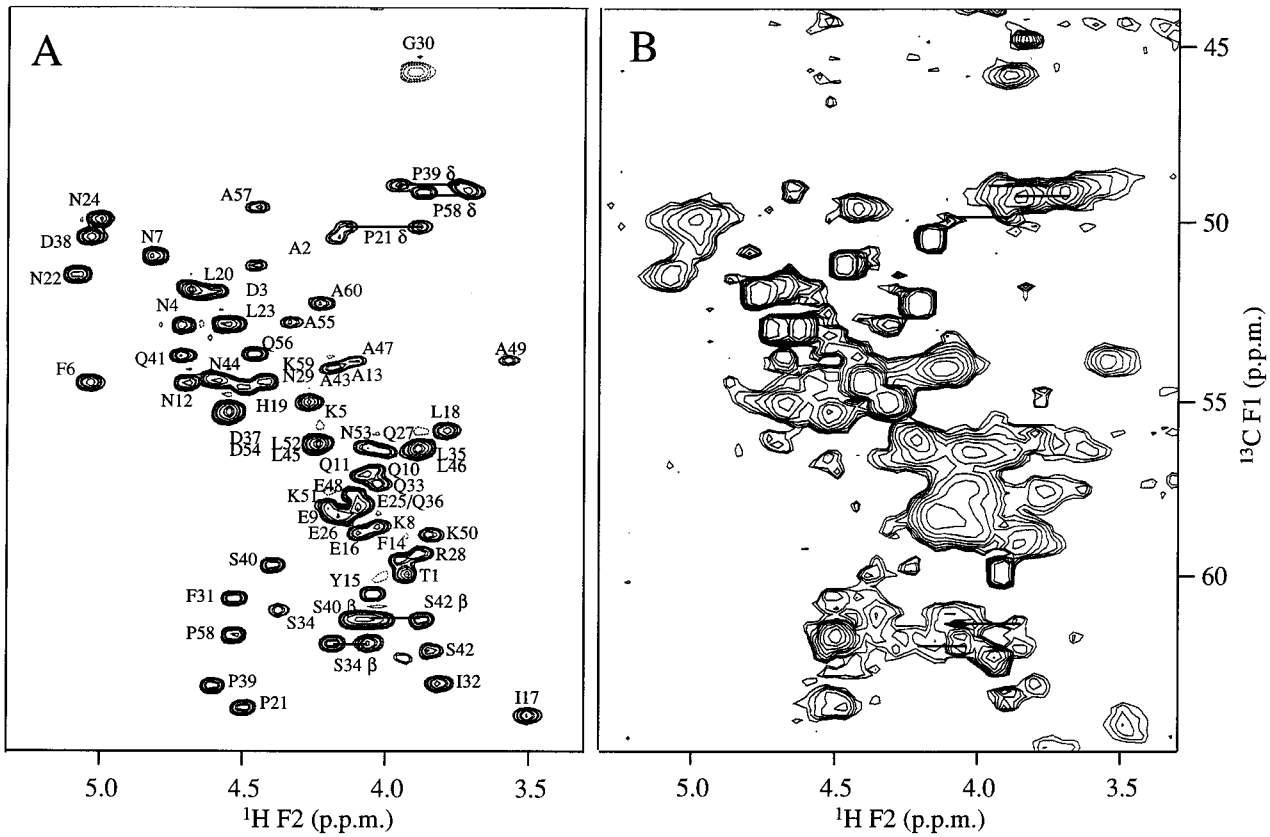

FIGURE 3: ^{13}Cα regions of ^{1}H−^{13}C HSQC spectra of [^{15}N/^{13}C]FB in the absence (A) and the presence (B) of 1 equiv of Fc at pH 6.0 and 42 °C. Cross-peaks connected by solid lines correspond to the resonances originating from the β-protons of serine or δ-protons of proline.

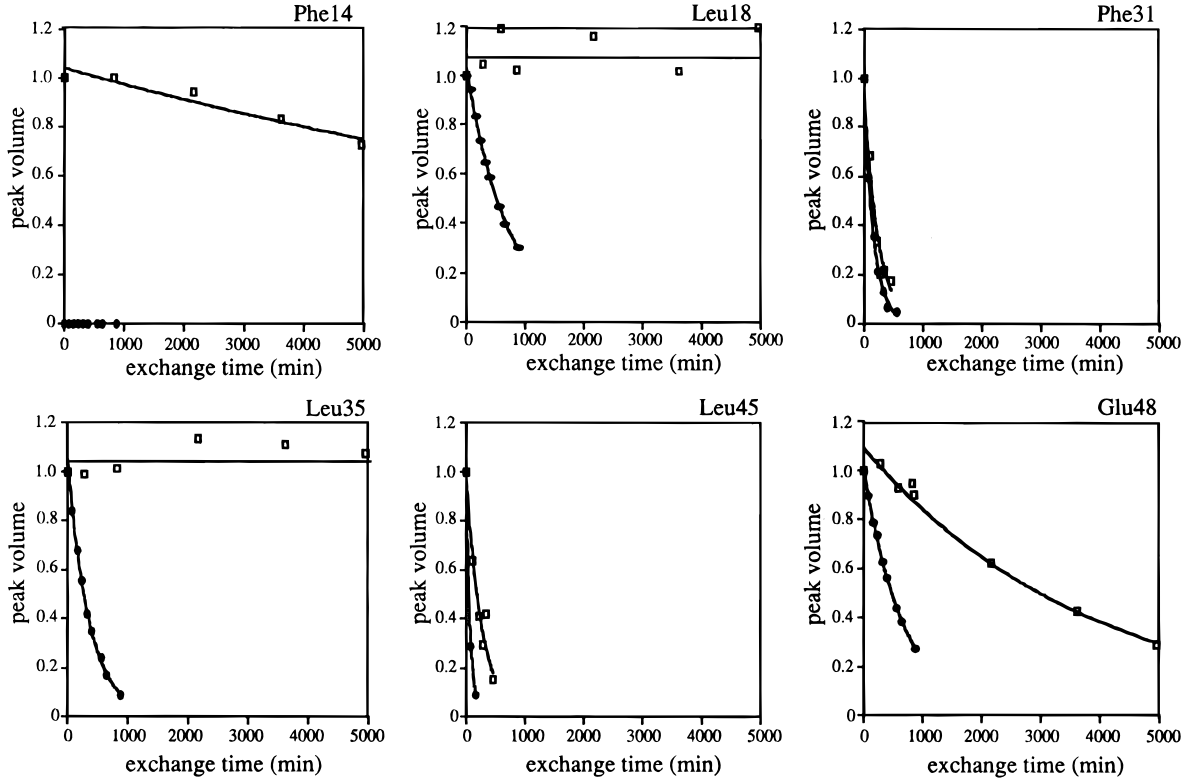

FIGURE 4: Representative H−D exchange curves in the free FB (closed circles) and the Fc-bound FB (open squares) at pH 6.0 and 30 °C. The normalized volumes for the ^{1}H−^{15}N HSQC cross-peaks are plotted as a function of the H−D exchange time.

resonances originating from helix III are affected by complex formation. These data along with the results obtained from ^{1}H−^{15}N HSQC spectra clearly indicate that helix III, which did not give any definite electron density in the X-ray structure, exists in the Fc-bound FB in solution.

Tashiro and Montelione (*19*) have recently pointed out the possibility that helix III is loosely packed compared with the other two helices in the presence of the Fc fragment,

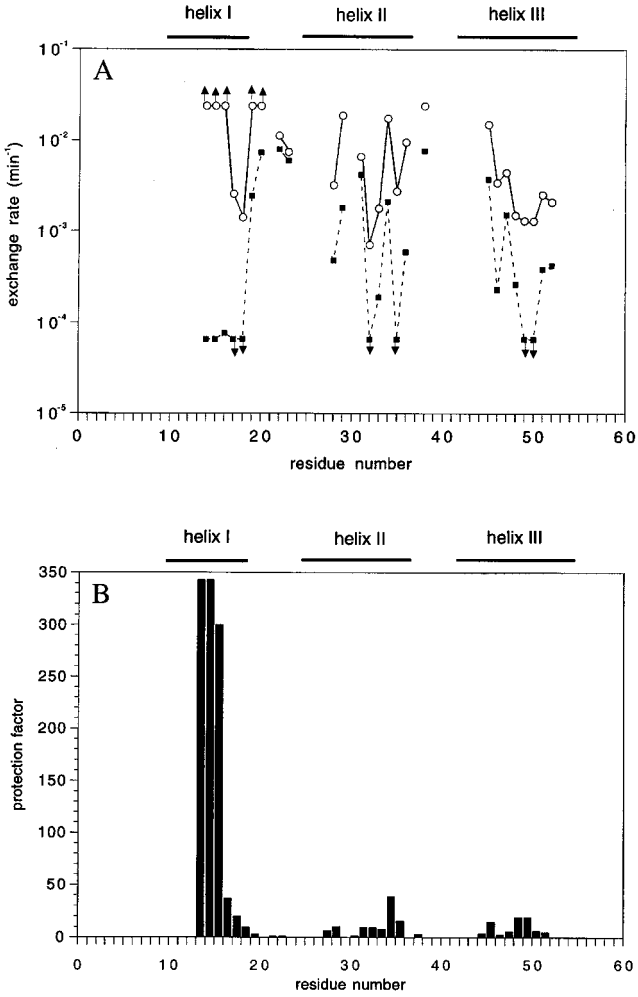

FIGURE 5: (A) Plots of k_{free} (open circles) and k_{bound} (closed squares) as a function of the residue number. Values for $(i)-(i+1)$ are connected by solid lines (free FB) or dashed lines (Fc-bound FB). (B) Protection factors at pH 6.0 and 30 °C as a function of the residue number. The α-helical regions are indicated by bars on top of the figures.

leading to the difference in the conformations of the Fc-bound FB in solution and in the crystal. This would indicate that the H−D exchange rates for the amide protons, which are located at the interface between helix III and helices I and II, significantly increase in the presence of the Fc fragment. However, as Figure 5A shows, in the presence of the Fc fragment, the H−D exchange rates for any amide protons are not faster than in the absence of the Fc fragment. We therefore conclude that the mode of packing of the three helices of FB does not change upon binding to the Fc fragment.

It has been demonstrated that FB makes two types of contact with Fc in the crystal of the FB−Fc complex (*5*). The crystal data have indicated that the first and second helical regions of FB and the C_H2 and C_H3 domains of the Fc fragment contribute to contact I (Table 2). It has also been shown that the second helical region and D38−Q41 that follow are covered by the formation of contact II (Table 2). We suggest that (1) the C-terminal region corresponding to helix III is in close spatial proximity to the C_H3 domain of the Fc fragment in the crystal, and (2) the crystal contact is the possible cause of the difference in the conformation of the C-terminal segment in solution and in the crystal.

Table 2: Comparison of Residues Involved in the Fc-Binding Site of FB Determined by H−D Exchange Experiments with Those by X-ray Crystal Study[a]

H−D exchange experiments	X-ray study	
	contact I	contact II
	F6	
	Q10	
	Q11	
	N12	
F14	F14	
Y15	Y15	
E16		
L18	L18	
H19	H19	
		E26
	R28	
N29	N29	N29
		G30
		F31
	I32	
Q33	Q33	Q33
		S34
L35		
K36	K36	K36
		D37
		D38
		P39
		S40
		Q41

[a] Deisenhofer, 1981.

Fc-Binding Site of FB in Solution. In order to discuss the Fc-binding site of FB in solution, we have carried out the H−D exchange and $^1H-^{15}N$ HSQC experiments. Combination of H−D exchange and 2D NMR has been used in the study of protein−protein interactions (*20*−*22*). It has been indicated that the H−D exchange rates for the amide protons of the main chain, which are buried in the interface of the protein−protein complex, are reduced when compared with the free protein. It has also been suggested that the residues with protection factors of 10 or larger form a contiguous surface and define the binding region in the proteins (*20*−*22*). Figure 6 represents the structure of FB with the side chains of residues which have protection factors of 10 or larger. On the basis of the solvent-accessible surface area calculated using the solution structure of FB, it is shown that of 14 residues shown in Figure 6, I17, I32, and A49 are completely buried in the hydrophobic core. This result suggests that Fc binding affects the dynamics of the global unfolding of FB, because the amide protons of these completely buried residues most likely exchange by unfolding of the protein. Other residues with a solvent-accessible surface area larger than 10 Å^2 are F14, Y15, E16, L18, H19, N29, Q33, L35, K36, L46, and K50. It is possible that these residues are also involved in Fc binding. The contiguous surface on FB is formed by these residues except for L46 and K50. Especially, F14, Y15, and E16 in helix I possess the highest protection factors of larger than 300 (Figure 5B). It has been shown that the magnitude of the highest protection factors obtained can be related to the binding affinity in terms of the relationship eq 1 (*20*):

$$k_{free}/k_{bound} = ([FB-Fc]/K_d)^{1/2} \quad (1)$$

Here [FB−Fc] is the concentration of the FB−Fc complex, and K_d is the dissociation constant of the complex. In the

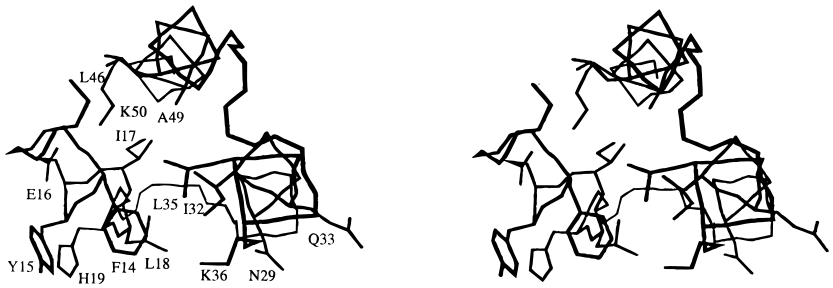

FIGURE 6: Stereopair of the solution structure of FB for the Q10−A55 segment. Side-chain atoms are shown for the residues with protection factors of 10 or larger.

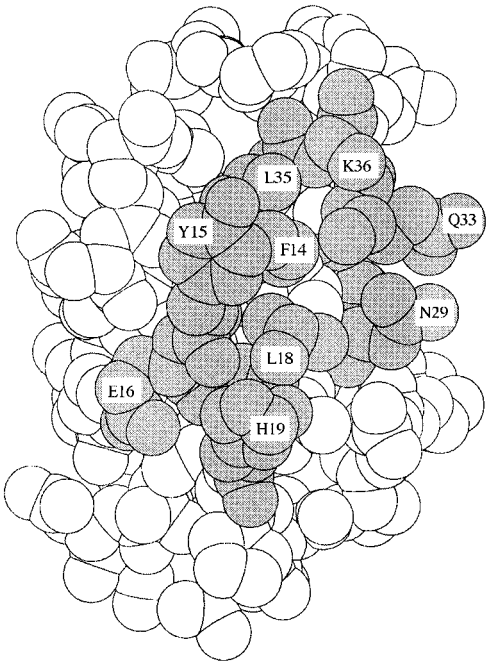

FIGURE 7: Space-filling representation of FB for the Q10−A55 segment. Numbers of the residues, which are identified to be part of the Fc-binding site from H−D experiment results, are indicated.

present experiment, [FB−Fc] is ~0.7 mM. On the basis of the protection factors obtained for F14, Y15, and E16, the binding constant between FB and Fc was estimated at $\sim 10^8$ M^{-1}. This value is consistent with that obtained using ^{125}I-labeled myeloma human IgG_1 (*1*). Therefore, we conclude that F14, Y15, and E16 significantly contribute to the Fc-binding site of FB. N29, Q33, L35, and K36, which are located on one side of helix II (Figure 6), have protection factors of 10 or larger. This indicates that the side of helix II, where N29, Q33, L35, and K36 are located, is involved in the Fc-binding site.

On the basis of the results of the H−D exchange experiments, we conclude that the surface region shaped by F14, Y15, E16, L18, and H19 in helix I and N29, Q33, L35, and K36 in helix II is responsible for the Fc-binding site of FB in solution (Figure 7). It should be noted that the core part of the binding site surrounded by the hydrophilic amino acid residues is composed of the hydrophobic residues (Figure 7).

We also prepared two mutants of FB: F14A and L18A, in which F14 and L18 are replaced by alanine residues, respectively (manuscript in preparation). Figure 8 shows the results of a competitive micro-ELISA experiment using FB, F14A, or L18A. The relative binding abilities of FB and its

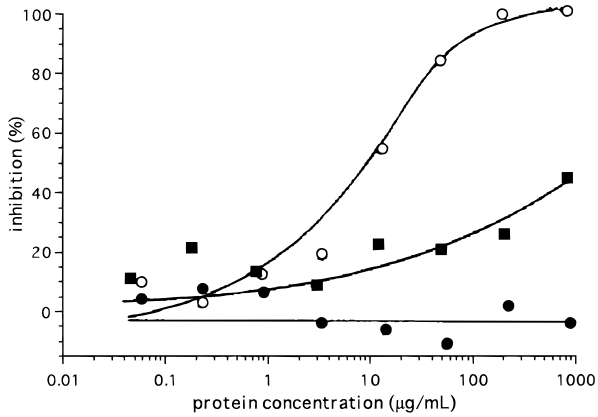

FIGURE 8: Inhibition curves obtained from the competitive micro-ELISA experiments. The open circles, closed circles, and closed squares indicate FB, F14A, and L18A, respectively.

mutants to the Fc fragment were determined in the competitive binding assay. It has been indicated that F14A does not bind at all to the Fc fragment and the binding ability of L18A is reduced to about 1% of that of FB. It has recently been reported that mutants of the Z domain, which is an analogue of FB, with a single amino-acid substitution at L18, N29, or K36 show a weakened binding to Fc compared with FB (*23*). All of these residues are involved in the Fc-binding site determined in the present study.

The residues that were suggested by the X-ray study (*5*) are summarized in Table 2. As shown in Table 2, the residues in the Fc-binding site determined by the present study significantly overlap with those from contact I. In view of the results of the NMR analyses reported in the present studies, we conclude that contact I is responsible for the formation of the FB−Fc complex in solution. On the basis of our previous observation that the amino acid residues of mouse Fc affected by the addition of FB are limited to those from contact I (*24*), the possibility of multiple binding of FB to the Fc fragment can be ruled out.

CONCLUSIONS

On the basis of the present NMR analyses, we conclude that in solution (1) helix III does exist in the FB−Fc complex, (2) the absence of electron density of helix III as observed in the X-ray structure is due to crystal contacts, (3) the contiguous surface shaped by F14, Y15, E16, L18, and H19 in helix I, and N29, Q33, L35, and K36 in helix II, is responsible for the Fc-binding of FB in solution.

REFERENCES

1. Langone, J. J. (1982) *Adv. Immunol. 32*, 157−252.
2. Sjödahl, J. (1977a) *Eur. J. Biochem. 73*, 343−351.

3. Sjödahl, J. (1977b) *Eur. J. Biochem. 78*, 471−490.
4. Moks, T., Abrahmsen, L., Nilsson, B., Hellman, U., Sjöquist, J., and Uhlén, M. (1986) *Eur. J. Biochem. 156*, 637−643.
5. Deisenhofer, J. (1981) *Biochemistry 20*, 2361−2370.
6. Gouda, H., Torigoe, H., Saito, A., Sato, M., Arata, Y., and Shimada, I. (1992) *Biochemistry 31*, 9665−9672.
7. Wishart, D. S., Sykes, B. D., and Richards, F. M. (1991) *J. Mol. Biol. 222*, 311−333.
8. Saito, A., Honda, S., Nishi, T., Koike, M., Ozaki, K., Itoh, S., and Sato, M. (1989) *Protein Eng. 2*, 481−487.
9. Torigoe, H., Shimada, I., Saito, A., Sato, M., and Arata, Y. (1990) *Biochemistry 31*, 8787−8793.
10. Grzesiek, S., and Bax, A. (1992) *J. Magn. Reson. 96*, 432−440.
11. Powers, R., Gronenborn, G., Clore, M., and Bax, A. (1991) *J. Magn. Reson. 94*, 209−213.
12. Marion, D., Ikura, M., Tschudin, R., and Bax, A. (1989) *J. Magn. Reson. 85*, 393−399.
13. Boudenhausen, G., and Ruben, D. J. (1980) *Chem. Phys. Lett. 69*, 185−189.
14. Vuister, G. W., and Bax, A. (1992) *J. Magn. Reson. 98*, 428−435.
15. States, D. J., Haberkorn, R. A., and Ruben, D. J. (1982) *J. Magn. Reson. 48*, 286−292.
16. Gronenborn, A. M., and Clore, G. M. (1993) *J. Mol. Biol. 233*, 331−335.
17. Wikström, M., Sjöbring, U., Drakenberg, T., Forsén, S., and Björck, L. (1995) *J. Mol. Biol. 250*, 128−133.
18. Bottomley, S. P., Popplewell, A. G., Scawen, M., Wan, T., Sutton, B. J., and Gore, M. G. (1994) *Protein Eng. 7*, 1463−1470.
19. Tashiro, M., and Motelione, G. T. (1995) *Curr. Opin. Struct. Biol. 5*, 471−481.
20. Paterson, Y., Englander, S. W., and Roder, H. (1990) *Science 249*, 755−759.
21. Mayne, L., Paterson, Y., Cerasoli, D., and Englander, S. W. (1992) *Biochemistry 31*, 10678−10685.
22. Zinn-Justin, S., Roumestand, C., Drevet, P., Menez, A., and Toma, F. (1993) *Biochemistry 32*, 6884−6891.
23. Cedergren, L., Andersson, R., Jansson, B., Uhlén, M., and Nilsson, B. (1993) *Protein Eng. 6*, 441−448
24. Kato, K., Gouda, H., Takaha, W., Yoshino, A., Matsunaga, C., and Arata, Y. (1993) *FEBS Lett. 328*, 49−54.

BI970923F